Metal Complexes in Inorganic Matrixes. 15.[1] Coordination of Metal Ions by Lysinate-Modified Titanium and Zirconium Alkoxides and the Preparation of Metal/Titania and Metal/Zirconia Nanocomposites

Ulrich Schubert,*[,†,‡] Stefan Tewinkel,[†] and Ryszard Lamber[§]

Institut für Anorganische Chemie der Technischen Universität Wien, Getreidemarkt 9, A-1060 Wien, Austria; Institut für Anorganische Chemie der Universität Würzburg, Am Hubland, D-97074 Würzburg, Germany; and Institut für Angewandte und Physikalische Chemie, Universität Bremen, Bibliotheksstrasse D-28359, Bremen, Germany

Received February 28, 1996. Revised Manuscript Received May 7, 1996[⊗]

The substituted metal alkoxides $(EtO)_3Ti$(lysinate) or $(BuO)_3Ti$(lysinate) are obtained when 1 equiv of lysine is added to $Ti(OEt)_4$ or $Zr(OBu)_4$. While the α-amino carboxylate moiety chelates the titanium or zirconium atom, the terminal amino group is capable of coordinating a metal ion. According to spectroscopic data, the complexes $(AcO)_2\{M[NH_2(CH_2)_4CH(NH_2)COO]E(OR)_3]_4\}$ (M = Co, Ni, Cu; E = Ti, Zr) are formed upon addition of $M(OAc)_2$ to ethanolic solutions of $(RO)_3E$(lysinate). The coordination of lysine and of the late transition metal ions is retained during sol−gel processing. There is no leaching of Co, Ni, or Cu ions from the metal complex-containing gels $(AcO)_2\{M[NH_2(CH_2)_4CH(NH_2)COO]EO_{3/2}]_4\}$. Upon oxidation of the gels in air at 500 °C, nanosized $CoTiO_3$ and $NiTiO_3$ particles in TiO_2, CuO particles in TiO_2, or MO particles in ZrO_2 were obtained. Subsequent reduction with hydrogen at 500 °C resulted in metallic nanoparticles dispersed in titania or zirconia. Composites of the same composition were prepared from unmodified $E(OR)_4$ and $M(OAc)_2$ for comparison. There is no systematic influence of the lysinate coordination on the metal particle size and size distribution of the final composites.

Introduction

We have previously developed a general method of preparing nanosized metal or alloy particles in SiO_2 matrixes by sol−gel processing, in which the metal particles are statistically distributed throughout the matrix and not agglomerated.[1−3] The main advantage is the very narrow size distribution of the metal particles. The key to achieve these properties is an atomic dispersion of the metal precursor during sol−gel processing. This is achieved by complexation of the metal compound and tethering the resulting metal complexes to the oxide matrix. Organofunctional alkoxysilanes of the type $(RO)_3Si(CH_2)_nA$ were used for this purpose. Groups A suitable for coordinating metal ions are, for example, NH_2, $NHCH_2CH_2NH_2$, CN, or $CH(COMe)_2$. In the second step of the preparation procedure, metal oxide particles are formed by oxidation of the metal-complex-containing gels in air under carefully controlled conditions. Because of the high dispersion of the metal precursor, very small metal oxide particles are formed which are then reduced to give the metal particles.

The transfer of the general conception to non-silicate systems was not possible, because suitable derivatives of the general type $(RO)_nE-X-A$, in which X is a hydrolytically stable spacer and A an organic group capable of coordinating metal ions, were not known for E ≠ Si. The functional group A cannot be linked to the alkoxide moiety by a hydrocarbon group, because of the hydrolytic cleavage of most relevant E−C bonds. Therefore, the grouping −X−A must have another chemical composition than for E = Si.

Complexing ligands (CL) have often been reported in the sol−gel literature as chemical additives to moderate the reactivity of non-silicate metal alkoxides. When the alkoxides are reacted with carboxylic acids, β-diketones, β-ketoesters, or related compounds (CL−H), part of the alkoxide groups is substituted by carboxylate or β-diketonate groups, etc. A new molecular precursor $E(OR')_y(CL)_x$ is obtained which exhibits a different molecular structure and reactivity. Upon addition of water, the alkoxy groups and not the complexing ligands are primarily hydrolyzed.[4] A second feature of complexing ligands is the possibility to control the cluster size of the primary hydrolysis products by the alkoxide:CL ratio.[5]

* To whom correspondence should be addressed at the Technical University of Vienna.
† University of Würzburg.
‡ Technical University of Vienna.
§ University of Bremen.
⊗ Abstract published in *Advance ACS Abstracts,* July 15, 1996.

(1) Part 14: Kaiser, A.; Görsmann, C.; Schubert, U. *J. Sol-Gel Sci. Technol.*, in press.

(2) (a) Breitscheidel, B.; Zieder, J.; Schubert, U. *Chem. Mater.* **1991**, *3*, 559. (b) Schubert, U.; Breitscheidel, B.; Buhler, H.; Egger, Ch.; Urbaniak, W. *Mater. Res. Soc. Symp. Proc.* **1992**, *271*, 621. (c) Mörke, W.; Lamber, R.; Schubert, U.; Breitscheidel, B. *Chem. Mater.* **1994**, *6*, 1659. (d) Schubert, U.; Schwertfeger, F.; Görsmann, C. In Chow, G.-M., Gonsalves, K., Eds.; *Molecularly Designed Nanostructured Materials, ACS Symp. Ser.* **1996**, *622*, 366.

(3) Schubert, U.; Görsmann, C.; Tewinkel, S.; Kaiser, A.; Heinrich, T. *Mater. Res. Soc. Symp. Proc.* **1994**, *351*, 141.

(4) Leading references: Sanchez, C.; Livage, J.; Henry, M.; Babonneau, F. *J. Non-Cryst. Solids* **1988**, *100*, 65. Sanchez, C.; Livage, J. *New J. Chem.* **1990**, *14*, 513.

(5) Chatry, M.; Henry, M.; In, M.; Sanchez, C.; Livage, J. *J. Sol-Gel Sci. Technol.* **1994**, *1*, 233.

S0897-4756(96)00162-7 CCC: $12.00

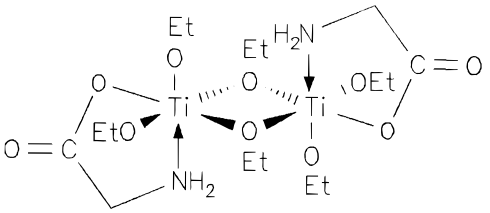

Figure 1. Structure of $\{(EtO)_3Ti[OOC\text{-}CH_2(NH_2)]\}_2$.

The complexing ligands can additionally be used for organic functionalization of sol−gel materials.[6] The most obvious choice are functionalized carboxylic acids, because they are readily available. Known compounds of the type $(R'O)_yE[OOC-Y-A]_x$, in which the functional group A is linked via the carboxylate group and some spacer Y to the metal alkoxide moiety, include (meth)acrylate,[7] chloro acetate,[8] and phosphanyl-substituted carboxylate derivatives[8] of $Ti(OR)_4$ or $Zr(OR)_4$. [Since the degree of association was not determined for most derivatives, monomeric formulas are given in this article. However, in most cases dimerization or oligomerization is highly probable.] We have recently shown that organofunctional sulfonic acids may serve the same purpose.[9]

The goal of the present work was 2-fold. First, we report on the use of lysinate-substituted titanium and zirconium alkoxides to coordinate transition-metal ions and on their use for the preparation of lysinate-modified titania and zirconia derivatives with ion-binding capability. A preliminary communication has appeared.[10] Second, we were investigating whether complexation of the metal ions and their tethering to the titanate or zirconate matrix has the same benevolent effect to the metal dispersion in the derived metal/TiO_2 or metal/ZrO_2 composites as in the case of silicate systems.

Results and Discussion

Modification of $M(OR)_4$ (M = Ti, Zr) by Amino Acids. Following the observation that pretreatment by alkyl titanates prevents wool from yellowing, several amino acids (glycine, alanine, leucine, phenylalanine, tyrosine, cysteine, methionine, and proline) were found to react with $Ti(OR)_4$. Elemental analysis indicated formation of the compounds $(RO)_3Ti[OOC-CH(NH_2)R']$.[11] The recent X-ray structure analysis of $(EtO)_3Ti[OOC-CH_2(NH_2)]$ showed the compound to be dimeric, with two bridging ethoxy groups (Figure 1). The α-amino group and one oxygen of the carboxyl group bind to the metal and form a five-membered chelate ring.[10] This kind of bonding considerably improves the hydrolytic stability of the aminocarboxylate ligand, compared with simple carboxylates.

The result of the structure analysis suggested that amino acids of the type $A-Y-CH(NH_2)COOH$, with a second functional group (A) in a more distant position, would be suitable to form precursors of the type $(R'O)_3M-X-A$ (M = Ti, Zr).

When lysine was added to an ethanolic solution of $Ti(OEt)_4$, the amino acid dissolved within 2 h, and a slightly yellow solution was obtained. The NH deformation vibration of the NH_3^+ group in lysine at 1516 cm^{-1} disappeared during the reaction, and bands at 3270 and 3125 cm^{-1} typical for NH_2 groups grew in. The carboxyl vibration shifted from 1584 to 1644 cm^{-1}. The compound was not isolated analytically pure because condensation reactions occurred during removal of the solvent, and the degree of association was not determined. However, the similarity of the solution IR spectrum with that of the structurally characterized glycinate derivative, particularly in the range of bridging and terminal OEt groups, is sufficient evidence that dimeric $[(EtO)_3Ti(lysinate)]_2$ (**1a**) was formed.

Lysine also dissolved in a propanolic solution of $Ti(OPr)_4$ or a butanolic solution of $Ti(OBu)_4$ upon heating to 60 °C. Since the same spectroscopic features were observed as in the reaction with $Ti(OEt)_4$, the coordination mode of the α-amino carboxylate appears to be the same in these derivatives. For the preparation of the metal/TiO_2 composites, we used only freshly prepared ethanolic solutions of **1a**.

The derivative $[(PrO)_3Zr(lysinate)]_x$ (**1b**) was similarly obtained by heating a propanolic solution of $Zr(OPr)_4$ with lysine. After removal of the solvent, a yellow solid was obtained. For the preparation of the composites, **1b** was prepared in ethanol, because this solvent is easier removed.

Formation of Metal Complexes. The availability of the terminal amino group in the lysine derivatives **1** was probed by reaction with metal salts. We used metal acetates, because the complete removal of the counterion is essential in the later stages of the composite preparation. When a solution of **1a** was treated with 0.25 equivalents of water-free $Co(OAc)_2$, the color of the solution changed to dark violet, and $Co(OAc)_2$ completely dissolved, indicating the formation of a metal complex. While $Co(OAc)_2$ in ethanol has a UV absorption maximum at 530 nm (both in the absence and the presence of $Ti(OEt)_4$), the maximum was shifted to 536 nm, when **1a** was employed. As expected for Co(II) complexes with amine ligands, the solution was sensitive to air, and the complex was destroyed by oxygen.

Upon reaction of a solution of **1a** with 0.25 equivalents of water-free $Ni(OAc)_2$, the color changed from green to blue while the salt dissolves. The UV absorption maximum of $Ni(OAc)_2$ in ethanol at 725 nm (both in the absence and the presence of $Ti(OEt)_4$) was shifted to 600 nm. The new position of the second maximum around 400 nm could not be identified, due to the intense absorptions of **1a** below 400 nm. The new absorption maximum is very similar to those of complexes between nickel halides and primary alkylamines.[12] For comparison, a solution of $Ni(OAc)_2$ and 4 equiv of *n*-butylamine in ethanol showed maxima at 384 and 636 nm.

The corresponding reactions of **1b** with $Co(OAc)_2$ and $Ni(OAc)_2$ similarly resulted in deep violet or blue solutions. The air-sensitive solution obtained with $Co(OAc)_2$ shows an absorption maximum at 512 nm (the Ni complex was too strongly opalescent).

We conclude from these observations that upon addition of the metal acetates to **1a,b** the complexes **2** and

(6) Schubert, U.; Hüsing, N.; Lorenz, A. *Chem. Mater.* **1995**, *7*, 2010.
(7) Schubert, U.; Arpac, E.; Glaubitt, W.; Helmerich, A.; Chau, C. *Chem. Mater.* **1992**, *4*, 291.
(8) Buhler, H.; Schubert, U. *Chem. Ber.* **1993**, *126*, 405.
(9) Barglik-Chory, C.; Schubert, U. *J. Sol-Gel Sci. Technol.* **1995**, *5*, 135. Lorenz, A.; Schubert, U. *Mater. Res. Soc. Symp. Proc.*, in press.
(10) Schubert, U.; Tewinkel, S.; Möller, F. *Inorg. Chem.* **1995**, *34*, 995.
(11) Lundgren, H. P.; Rose, W. G.; Walden, M. K. *J. Org. Chem.* **1961**, *26*, 1467.
(12) Uhlig, E.; Staiger, K. *Z. Anorg. Allg. Chem.* **1965**, *336*, 42.

3 are formed (eq 1). Whether acetate is coordinated to the metal cannot be decided. However, this question is irrelevant to the composite synthesis.

1a + $M(OAc)_2$ →

$(AcO)_2\{M[NH_2(CH_2)_4CH(NH_2)COO]E(OR)_2X]_4\}$ (1)

	M	E	R	X
2a	Co	Ti	Et	OEt
3a	Ni	Ti	Et	OEt
4a	Cu	Ti	Et	OAc
2b	Co	Zr	Pr	OPr
3b	Ni	Zr	Pr	OPr
4b	Cu	Zr	Pr	OAc

Reaction of **1a,b** with 0.25 equiv of $Cu(OAc)_2 \cdot H_2O$ resulted in deep green-blue solutions. To achieve a sufficient solubility of the resulting copper complexes 1 equiv of acetic acid had to be added. Since acetic acid reacts with $E(OR)_4$ (E = Ti, Zr) by substitution of one OR ligand for acetate,[4] the resulting complexes **4** presumably have the composition $(AcO)_2\{Cu[NH_2(CH_2)_4CH(NH_2)COO]E(OR)_2(OOCCH_3)]_4\}$. The solutions were slightly opaque, probably due to partial hydrolysis by the crystal water. Therefore, no UV spectra were obtained.

Hydrolysis of the M(OR)$_3$(lysinate)-Substituted Metal Complexes. Precipitates were formed when water was added to concentrated solutions of the complexes **2** and **3**. This can either be avoided by adding acetic acid or by working with rather dilute solutions. In the present work, sol−gel processing was carried out at 60 °C by addition of 7.5 mol equiv (per OR group) of water to 0.02 M ethanolic solutions of **2**−**4**. Within 72 h, the solutions became opaque, but there was no precipitate. Removal of the solvent and drying resulted in xerogels, which could not be redissolved in ethanol. In all cases the specific surface area was below 4 m^2/g. Elemental analyses indicated (within the accuracy for such systems) that hydrolysis and condensation was complete and that the compounds **5**−**7** had the anticipated composition (eq 2).

2,3 $\xrightarrow{+H_2O}$

$(AcO)_2\{M[NH_2(CH_2)_4CH(NH_2)COO]EO_{3/2}]_4\}$ (2a)

	M	E
5a	Co	Ti
6a	Ni	Ti
5b	Co	Zr
6b	Ni	Zr

4 $\xrightarrow{+H_2O}$

$(AcO)_2\{Cu[NH_2(CH_2)_4CH(NH_2)COO]TiO(OAc)]_4\}$ (2b)

7a: E = Ti, **7b**: E = Zr

The xerogels had the same colors as the solutions of the M(OR)$_3$(lysinate)-substituted metal complexes **2**−**4**. Therefore, one can conclude that the Ni, Co, or Cu ions are still coordinated in the same way as in solution, i.e., formation of the titanate or zirconate matrix does not affect the coordination of the metal ions. This was spectroscopically confirmed for **6a**. The solid-state UV spectrum of **6a** is very similar to that of **3a** in solution with an absorption maximum at 616 nm. In the infrared spectra of the compounds **5**−**7** the COO vibration of the aminocarboxylate group is still around 1635 cm^{-1}. This observation strongly suggests that this group is still coordinated to titanium or zirconium.

Cleavage of the aminocarboxylate group during sol-gel processing would result in the typical COOH vibrations of lysine, which are not observed. There was no elution of either metal ions or lysine when the xerogels **5**−**7** were washed with water. The composition of the solids was the same before and after washing.

The combined evidence strongly suggests that during sol−gel processing of the complexes **3**−**5** neither the Ti-(Zr)−carboxylate link nor the coordination of the metal ions to the terminal amino group of the lysinate derivative is broken. The metal ions are therefore tightly tethered to the titanate or zirconate matrix. This is schematically shown in Scheme 1 (left) for **6a**. The lysinate derivatives **1** are therefore equivalent to the aminoalkyl*silane* derivatives $(RO)_3Si(CH_2)_3NR'_2$ (e.g., $NR_2 = NH_2$, $NHCH_2CH_2NH_2$), which were, inter alia, used for tethering metal ions to the *silicate* matrix during the preparation of metal/SiO_2 nanocomposites (Scheme 1, right).[2]

For comparison, samples with the same 1:4 ratio between M (Ni, Co, Cu) and E (Ti, Zr) were prepared by sol−gel processing of $E(OR)_4$ and the metal acetates *without* using lysine (eq 3). The experimental conditions were exactly the same (only the water ratio was adjusted to the greater number of alkoxide groups per Ti or Zr atom). The samples are labelled **5**−**7(o)** ("o" = without lysine). Contrary to the samples prepared from **2**−**4**, hydrolysis was very incomplete, indicated by the high carbon content in the elemental analyses. There was extensive leaching of the metal ions, when the xerogels **5**−**7(o)** were treated with water.

$4E(OR)_4 + M(OAc)_2 + 8H_2O \rightarrow M(OAc)_2/4\ EO_{2-0.5x}(OR)_x + \ldots$ (3)

	M	E	R
5a(o)	Co	Ti	Et
6a(o)	Ni	Ti	Et
7a(o)	Cu	Ti	Et
5b(o)	Co	Zr	Pr
6b(o)	Ni	Zr	Pr
7b(o)	Cu	Zr	Pr

Oxidation of the Xerogels 5−7. In this step all organic groupings have to be completely removed by heat treatment in air. At the same time the metal ions aggregate to form small oxide particles in the gel matrix. As previously shown for silicate systems, this step has to be carefully optimized, because it determines the metal particle size and size distribution of the composites.[1,13] Oxidation by pure oxygen is too exothermic, and therefore heating the gels in air allows a better control of this step. The temperature has to be high enough to allow the complete removal of all organic groups (i.e., the lysinate group, and the acetate ions used as counterions or for the modification of the Cu-containing systems).

Thermogravimetric analysis of the metal complex containing gels **5**−**7** showed the oxidative decomposition

(13) Görsmann, C. Ph.D. Thesis, Universität Würzburg, Germany, 1996.

Scheme 1

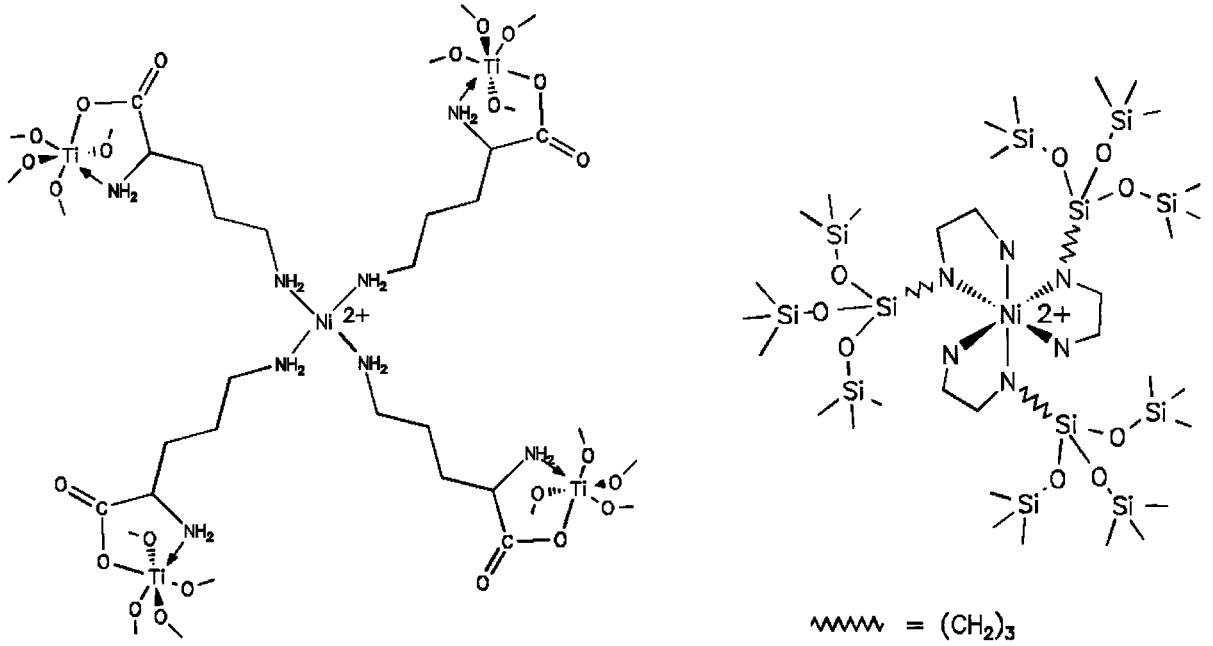

to be finished at about 450 °C. For the preparative scale oxidations we therefore heated the gels to 500 °C by 10 °C/min and then held them at 500 °C for 2 h. Elemental analysis of the products showed that carbon, hydrogen, and nitrogen were completely removed.

The composition of the gels was analyzed by X-ray diffraction (XRD). The reflexions in the XRD spectrum of the green powder obtained by oxidation of the Co-containing xerogel **5a** could be assigned to rutile (JCPDS 211276), anatase (weak reflexions, JCPDS 211272), and cobalt titanate (strong reflexions, JCPDS 150866) (eq 4a). The latter explains the green color of the

$$\mathbf{5a, 6a} + O_2 \rightarrow \underset{\mathbf{8a}:\ M = Co;\ \mathbf{9a}:\ M = Ni}{MTiO_3/3TiO_2 + \cdots} \qquad (4a)$$

composite. If oxidation is carried out at 600 °C, only the rutile phase was observed for TiO_2, at oxidation temperatures below 450 °C only anatase. The XRD spectrum of the yellow powder obtained by oxidation of the Ni-containing xerogel **6a** is very similar. Rutile, anatase, and nickel titanate (JCPDS 330960) were identified. Contrary to the Co-containing composite, anatase was the dominant phase, and the reflections of rutile were rather weak. There were no reflections for cobalt or nickel oxides; however, we of course cannot exclude the presence of amorphous oxide phases.

The reflections of the black powder obtained by air-oxidation of **7a** could be assigned to CuO (tenorite, JCPDS 410254) and anatase (eq 4b). No rutile phase was found.

$$\underset{\mathbf{10a}}{\mathbf{7a}} + O_2 \rightarrow CuO{\cdot}4TiO_2 + \cdots \qquad (4b)$$

To determine the influence of the metal complexation by lysine on the development of the different phases and on the particle sizes and size distributions, we also prepared the composites $CoO/4TiO_2$ (**8a(o)**), $NiO/4TiO_2$ (**9a(o)**), and $CuO/4TiO_2$ (**10a(o)**) starting from **5a(o)**−**7a(o)**. The reaction conditions were identical to make the products comparable. The XRD reflections of **8a(o)**−**10a(o)** are given in Table 2.

Table 1. *d* Spacings of the Oxidation Products of 8a−10a [Å] (Assignments Made in Comparison with the Spectra in the JCPDS Data Base)

8a		**9a**		**10a**[a]	
3.712	$CoTiO_3$	3.644	$NiTiO_3$	3.481	anatase
3.521	anatase	3.500	anatase	2.507	CuO
3.249	rutile	3.235	rutile	2.418	anatase
2.726	$CoTiO_3$	2.698	$NiTiO_3$/rutile	2.366	anatase
2.531	$CoTiO_3$	2.507	$NiTiO_3$/rutile	2.315	CuO
2.491	rutile	2.377	anatase	1.889	anatase
2.376	anatase	2.198	$NiTiO_3$	1.861	CuO
2.311	anatase	2.085	NiO/rutile	1.695	anatase
2.222	$CoTiO_3$	1.897	anatase	1.663	anatase
2.184	rutile	1.844	$NiTiO_3$	1.580	CuO
2.057	rutile	1.697	anatase/rutile	1.502	CuO
1.892	anatase	1.483	$NiTiO_3$	1.479	anatase
1.856	$CoTiO_3$	1.449	$NiTiO_3$	1.405	CuO
1.711	$CoTiO_3$				
1.688	rutile				
1.620	rutile				
1.495	anatase				
1.461	$CoTiO_3$				

[a] The values are slightly shifted due to an instrumental error.

Table 2. *d* Spacings of the Composites 8a(o)−10a(o) [Å] (Assignments Made in Comparison with the Spectra in the JCPDS Data Base)

8a(o)		**9a(o)**		**10a(o)**	
3.661	$CoTiO_3$	3.492	anatase	3.513	anatase
3.470	anatase	3.235	rutile	2.520	CuO
3.197	rutile	2.698	$NiTiO_3$	2.426	anatase
2.709	$CoTiO_3$	2.486	rutile/$NiTiO_3$	2.370	anatase
2.516	$CoTiO_3$	2.187	rutile/$NiTiO_3$	2.329	CuO
2.359	anatase	1.894	anatase	1.894	anatase
2.212	$CoTiO_3$	1.844	$NiTiO_3$	1.697	anatase
2.174	rutile	1.689	anatase/rutile	1.669	anatase
1.888	anatase	1.467	$NiTiO_3$	1.479	anatase
1.851	$CoTiO_3$	1.448	$NiTiO_3$		
1.705	$CoTiO_3$				
1.674	rutile				
1.616	rutile				
1.493	anatase				
1.479	$CoTiO_3$				
1.458	$CoTiO_3$				

In **8a(o)**−**10a(o)** the same phases were identified as the composites **8a**−**10a** prepared with lysine. The anatase:rutile ratio in **8a(o)** and **9a(o)** was higher than

Table 3. Average Particle Sizes [nm] in the Composites 8a−10a and 8a(o)−10a(o), Determined from the XRD Line Widths

	anatase	rutile	$MTiO_3$ (M = Co, Ni) or CuO
8a	16	16	47
8a(o)	27	8	28
9a	11	12	22
9a(o)	16	6	7
10a	25		61
10a(o)	37		8

Scheme 2

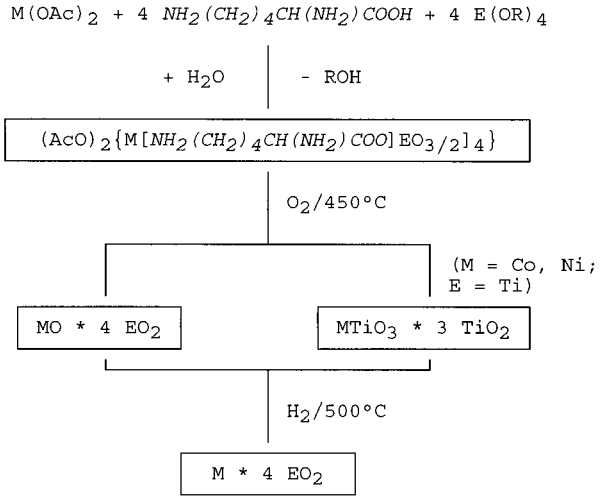

in **8a** and **9a**. **9a(o)** was somewhat inhomogeneous. The main difference between the composites prepared with or without lysine was the width of the reflections. In the composites **8a(o)**−**10a(o)**, most reflexions are weaker and broader than in **8a**−**10a**, indicating smaller particle sizes of both the TiO_2 phase and the metal oxide or titanate phase. The average particle sizes calculated from the line broadening of the XRD reflections by Scherrer's equation[14] are given in Table 3. The use of lysine for the complexation of the late transition metal ions generally results in smaller anatase particles but larger rutile and metal oxide (metal titanate) particles.

XRD analysis of the composites **8b**−**10b** obtained by air-oxidation of the metal-complex-containing *zirconate* gels **5b**−**7b** was less straightforeward, because the reflections of **8b** and **9b** were very broad. In all cases cubic ZrO_2 was identified. An additional reflection in the spectrum of **9b** at 2.093 Å was assigned to NiO, and the reflection at 2.320 Å in the spectrum of **10b** to CuO (eq 5). There was no additional crystalline phase in the Co-containing gel (the formula for **8b** therefore is tentative).

$$\mathbf{5b}-\mathbf{7b} + O_2 \rightarrow MO{\cdot}4ZrO_2 + \cdots \quad (5)$$

8b: M = Co; **9b**: M = Ni; **10b**: M = Cu

Composites of the same overall composition prepared without lysine (**8b(o)**−**10b(o)**) exhibited the same features; the XRD bands were even broader than in the composites **8b**−**10b**.

Reduction of the Composites 8−10. In the final step of the synthesis of the metal/TiO_2 and metal/ZrO_2 composites (Scheme 2) the metal oxide or metal titanate particles obtained in the previous step were reduced by hydrogen. The gels were heated to 500 °C by 10 °C/min and then held at 500 °C for 2 h in a stream of hydrogen.

(14) Scherrer, P. *Gött. Nachr.* **1918**, *2*, 98.

Table 4. *d* Spacings of the Composites 11a−13a [Å] (Assignments Made in Comparison with the Spectra in the JCPDS Data Base)

11a		**12a**		**13a**	
3.516	anatase	3.486	anatase	3.510	anatase
3.242	rutile	3.249	rutile	2.428	anatase
2.478	rutile	2.482	rutile	2.379	anatase
2.293	rutile	2.367	anatase	2.333	anatase
2.182	rutile	2.297	rutile	2.088	Cu
2.041	Co	2.185	rutile	1.893	anatase
1.895	anatase	2.040	Ni	1.808	Cu
1.686	rutile	1.895	anatase	1.699	anatase
1.624	rutile	1.765	Ni	1.667	anatase
1.478	rutile	1.688	rutile	1.480	anatase
1.452	rutile	1.627	rutile		
		1.477	rutile/anatase		
		1.450	rutile		

Table 5. *d* Spacings of the Composites 11b−13b [Å] (Assignments Made in Comparison with the Spectra in the JCPDS Data Base)

11b		**12b**		**13b**	
2.922	ZrO_2	2.924	ZrO_2	2.947	ZrO_2
2.547	ZrO_2	2.528	ZrO_2	2.545	ZrO_2
2.075	Co	2.052	Ni	2.084	Cu
1.798	ZrO_2	1.801	ZrO_2	1.803	ZrO_2
1.530	ZrO_2	1.536	ZrO_2	1.533	ZrO_2
1.467	ZrO_2	1.468	ZrO_2	1.473	ZrO_2

The reflections of the metal oxide or metal titanate particles were no longer observed in the XRD spectra of the reduced composites **11**−**13** (Table 4 and 5). Instead, the reflections of the corresponding elemental metals were observed (eq 6). The reflections of Co in

$$\mathbf{8}-\mathbf{10} + H_2 \rightarrow M{\cdot}4EO_2 + H_2O \quad (6)$$

	M	E
11a	Co	Ti
12a	Ni	Ti
13a	Cu	Ti
11b	Co	Zr
12b	Ni	Zr
13b	Cu	Zr

the ZrO_2 composite **11b** were very weak and broad. In the composites **11a** and **12a**, the anatase:rutile intensity ratio was further decreased, while in **13a** only the anatase phase was present. The crystallinity of the ZrO_2 phase was distinctly improved, and sharp reflections were observed in all composites.

The corresponding composites **11(o)**−**12(o)** were obtained by the same procedure (XRD data in Table 6 and 7). In the case of **13a(o)** reduction at the standard conditions was not complete, since weak reflections of CuO were still observed. The reflections of Co in **11b(o)** and Cu in **13b(o)** were very weak.

The average metal particle sizes calculated from the line broadening of the XRD reflections are given in Table 8. An interesting feature is the redispersion of the Co and Ni particles in **11a** and **12a** during reduction, i.e., a decreased size relative to their titanate precursors (**8a** and **9a**). This effect is not observed for the composites prepared without lysine and for the Cu-containing composite **13a**.

We have recently shown for Cu/Ni particles dispersed in SiO_2 that complexation and tethering of the metal ions in the sol−gel stage does not necessarily lead to

Table 6. *d* Spacings of the Composites 11a(o)−13a(o) [Å] (Assignments Made in Comparison with the Spectra in the JCPDS Data Base)

11a(o)		12a(o)		13a(o)	
3.519	anatase	3.508	anatase	3.513	anatase
3.254	rutile	3.249	rutile	2.524	CuO
2.489	rutile	2.481	rutile	2.435	anatase
2.433	anatase	2.370	anatase	2.376	anatase
2.380	anatase	2.299	rutile	2.335	anatase
2.333	anatase	2.185	rutile	2.095	Cu
2.187	rutile	2.040	Ni	1.894	anatase
2.044	Co	1.895	anatase	1.822	Cu
1.893	anatase	1.765	Ni	1.698	anatase
1.686	rutile/anatase	1.685	rutile	1.666	anatase
1.631	rutile	1.626	rutile	1.480	anatase
1.480	rutile/anatase	1.479	rutile/anatase		
		1.451	rutile		

Table 7. *d* Spacings of the Composites 11b(o)−13b(o) [Å] (Assignments Made in Comparison with the Spectra in the JCPDS Data Base)

11b(o)		12b(o)		13b(o)	
2.930	ZrO_2	2.943	ZrO_2	2.915	ZrO_2
2.536	ZrO_2	2.545	ZrO_2	2.522	ZrO_2
2.066	Co	2.052	Ni	2.114	Cu
1.794	ZrO_2	1.801	ZrO_2	1.796	ZrO_2
1.529	ZrO_2	1.536	ZrO_2	1.529	ZrO_2
1.468	ZrO_2	1.471	ZrO_2	1.466	ZrO_2

Table 8. Average Particle Sizes [nm] in the Composites 11−13 and 11(o)−13(o), Determined from the XRD Line Widths

	anatase	rutile	ZrO_2	M
11a	13	15		19
11a(o)	28	11		27
12a	18	16		11
12a(o)	17	15		12
13a	17			53
13a(o)	38			13
11b			7	*a*
11b(o)			9	*a*
12b			8	7
12b(o)			17	25
13b			7	20
13b(o)			14	*a*

[a] Reflections too weak.

smaller metal particles. However, narrower particle size *distributions* are obtained.[1] To find out whether this is also true for the TiO_2- and ZrO_2-based composites we exemplarily investigated the composites **12a**, **12a(o)**, and **12b** by transition electron microscopy (TEM). Bright-field and dark-field images are shown in Figures 2−4, and the corresponding particle size distributions in Figures 5−7. In both in the dark-field and the bright-field image of **12a**, some moiré figures are visible. They are due to interference between beams diffracted through Ni and TiO_2. The Ni(111) reflection was used for dark-field imaging; the Ni crystallites are visible as bright spots. Microdiffraction analysis of Ni crystallites on TiO_2 did not give any evidence for epitaxial growth of Ni on the TiO_2 matrix.

Conclusions

The modification of titanium and zirconium alkoxides with lysine results in derivatives with cation-coordinating capability. They can be employed for the preparation of titanate or zirconate materials which can bind metal ions. Leaching experiments showed that both the bond of the aminocarboxylate group to titania or zirconia and the coordination of the metal ions to the terminal amino group of the lysinate ligand are sufficiently strong. The lysinate derivatives **1a,b** therefore can be used in the same way as the alkoxysilane derivatives $(RO)_3SiCH_2CH_2CH_2NR_2$, for which many applications exist.

The process for the preparation of the metal/TiO_2 and metal/ZrO_2 nanocomposites with the help of the lysinate derivatives **1a,b** is summarized in Scheme 2. It should be pointed out that the metal contents of the composites could be lowered to any concentration by increasing the amount of $Ti(OR)_4$ or $Zr(OR)_4$ in the starting mixture, i.e., by using a mixture of $E(OR)_4$ and the lysinate derivatives **1** in any ratio.

When metal/SiO_2 derivatives are prepared by using the alkoxysilane derivatives $(RO)_3SiCH_2CH_2CH_2NR_2$, complexation and tethering of the metal ions during sol−gel processing in every case investigated so far had a very positive influence on the particle size distribution and mostly also on the average particle size in the final composites. The results presented in this paper show that the use of the lysinate derivatives has no comparable influence on the size and size distribution of metal particles dispersed in TiO_2 or ZrO_2. The metal oxide or metal titanate particles in TiO_2 are significantly smaller when no lysine is used during sol−gel processing. Some redispersion of the metal is observed upon reduction of $NiTiO_3$ or $CoTiO_3$. There is no clear picture for the ZrO_2-based composites, because in most composites the XRD reflections were to broad for a particle size analysis. The available data indicate no systematic influence of lysine on the metal oxide or metal particle sizes.

The particle size distribution was exemplarily investigated for **12a** (Figure 4), **12a(o)** (Figure 5) and **12b** (Figure 6). In each case the size distribution is regular and rather narrow. In composite **12a(o)**, prepared without lysine, it is only insignificantly narrower than that of **12a** prepared from $(EtO)_3Ti$(lysinate). One reason for the missing influence of the metal coordination by the lysinate derivative may be that the size distribution of **12a(o)** is already narrow. Therefore, the use of **1a** may give no significant improvement.

Surprisingly, the use of the lysinate derivative *does* influence the average crystallite size of the matrix. There is a distinct decrease of the average particle size of the anatase or ZrO_2 matrix in most cases investigated in this paper. Only the size of the rutile crystallites appears to be uninfluenced. We currently have no explanation for this phenomenon which we will further investigate.

The dependency of the anatase:rutile ratio on the kind of late transition metal in the preparation of the composites **8**−**10** under identical temperature conditions is an interesting side aspect of this work.

Experimental Section

General Methods. All operations involving metal alkoxides were carried out under an atmosphere of dry N_2 using conventionally dried solvents. The alkoxides, lysine, and $Cu(OAc)_2 \cdot H_2O$ were used as received. $Ni(OAc)_2$ and $Co(OAc)_2$ were obtained by drying the dihydrates at 100 °C in vacuo until no further weight loss occured. IR spectra: Bruker FTIR IF S25. NMR spectra: Bruker AC 200. UV−vis solution spectra: Perkin-Elmer Lambda 15 and Hewlett-Packard 8452 A. UV solid-state spectra: Shimadzu UV 3100 with an integrating sphere MPC 3100. TGA and DSC: DuPont thermal analyzer 9000. BET measurements: Micromeritics

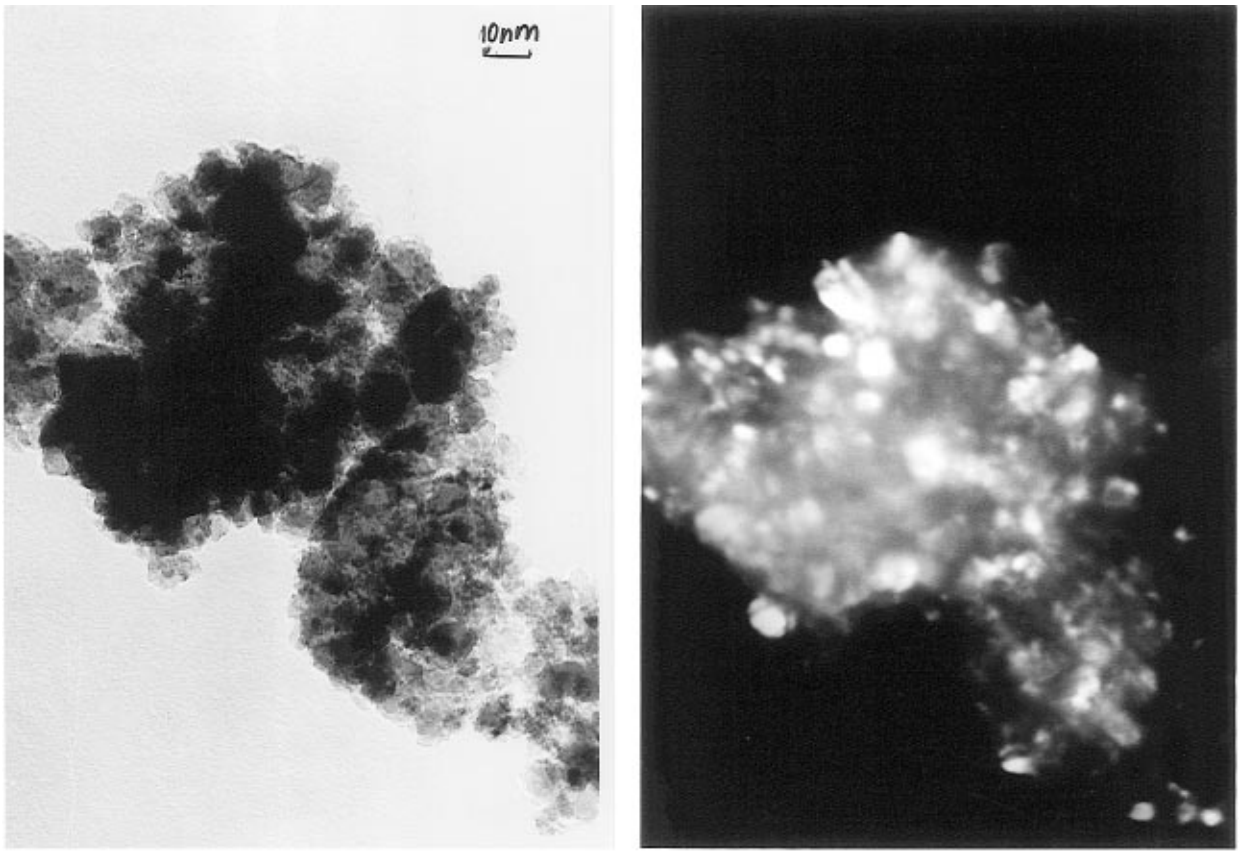

Figure 2. Electron micrographs of Ni·4TiO_2 (**12a**). (a) Bright field. (b) Dark-field image obtained with the Ni(111) reflection. Both pictures are on the same scale.

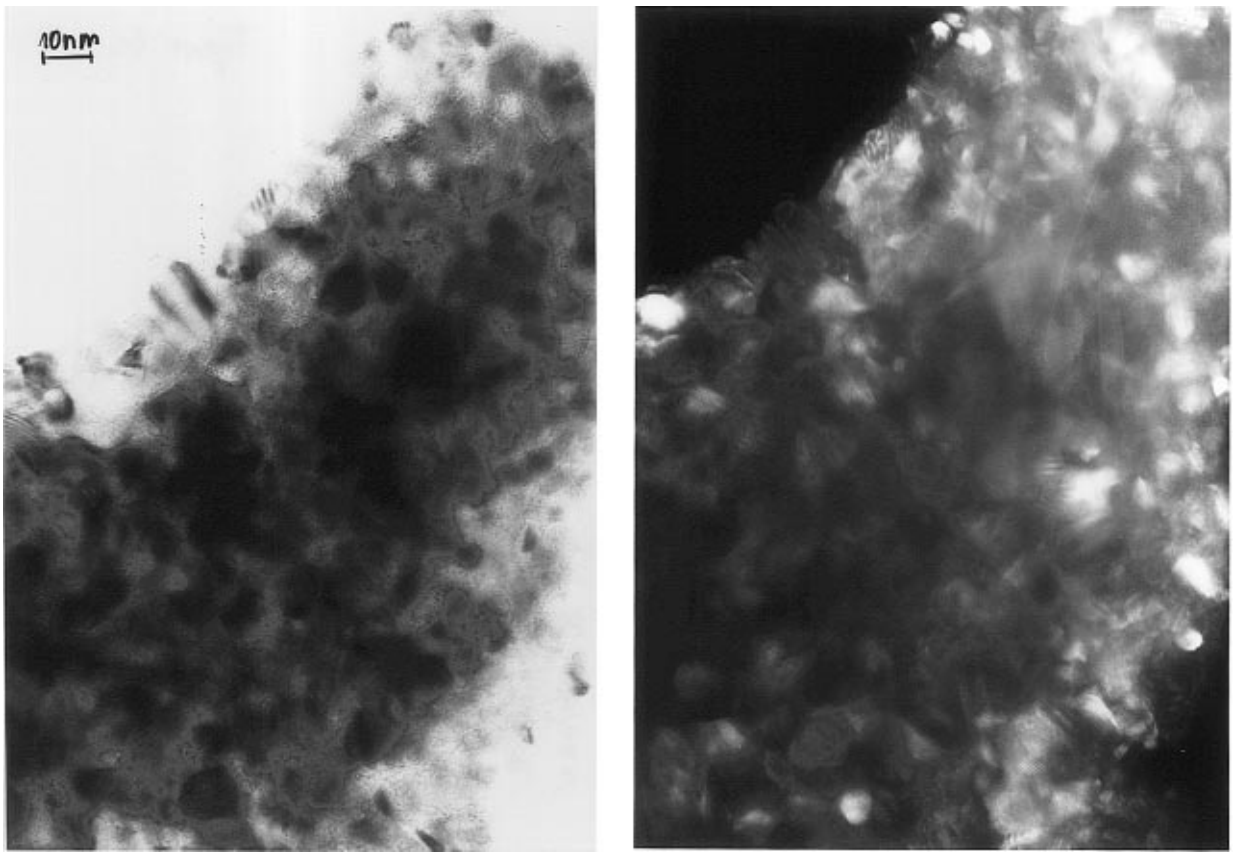

Figure 3. Electron micrographs of Ni·4TiO_2 (**12a(o)**). (a) Bright field. (b) Dark-field image obtained with the Ni(111) reflection. Both pictures are on the same scale.

ASAP 2400 (N_2 adsorption). Before the determination of the specific surface area, the samples were grinded in an agate mortar and degassed at 110 °C/0.01 Torr for 16 h.

XRD: Philips 1050. The samples were grinded in an agate mortar. The 2θ values were converted into d spacings by Bragg's equation and then compared with the data in the

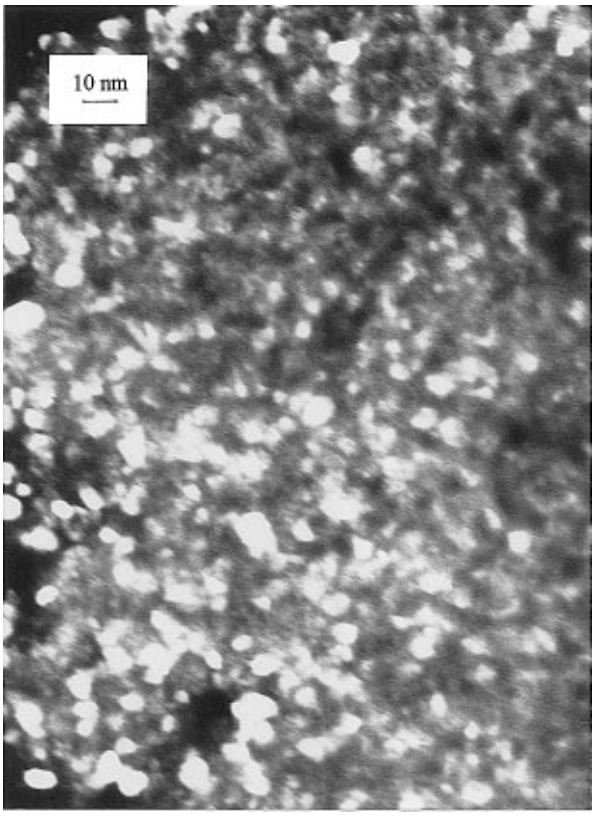

Figure 4. Electron micrographs of Ni·4ZrO_2 (**12b)**. Dark-field image obtained with the Ni(111) reflection.

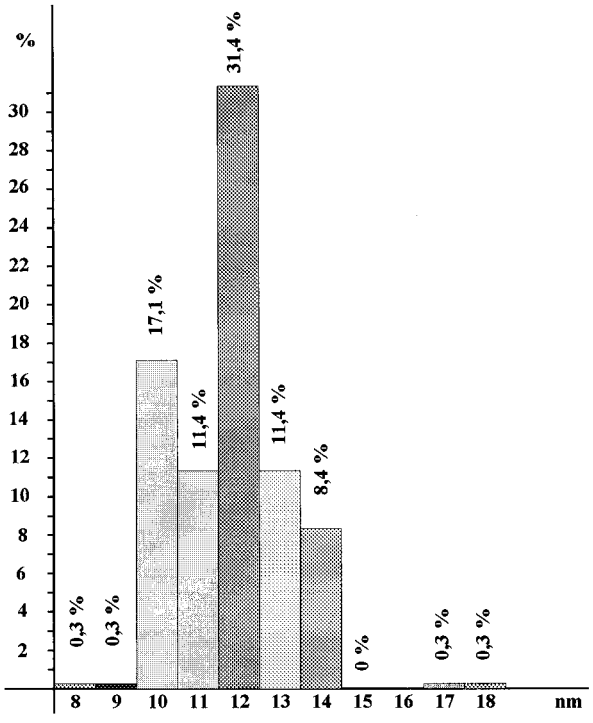

Figure 5. Ni particle size distribution of Ni·4TiO_2 (**12a**), prepared from $Ni(OAc)_2$ and $(EtO)_3$Ti(lysinate).

JCPDS data base (Table 9). For the determination of the average particle sizes from the line widths the following reflections were chosen: rutile $2\theta = 27.5°$, anatase $2\theta = 25.4°$, $CoTiO_3$ $2\theta = 32.8°$, $NiTiO_3$ $2\theta = 33.1°$, CuO $2\theta = 35.7°$.

Transition electron microscopy (TEM) was carried out with a Philips EM 420T electron microscope operated at 120 kV and equipped with an energy-dispersive X-ray analyzer (EDX). The samples were ground to a fine powder, deposited on Cu grids coated with a carbon film, and dispersed on the grid ultrasonically. No organic solvents were used during this procedure.[2c] Tilted beam illumination was used for dark-field imaging. The particle size distributions were determined from 100−500 particles.

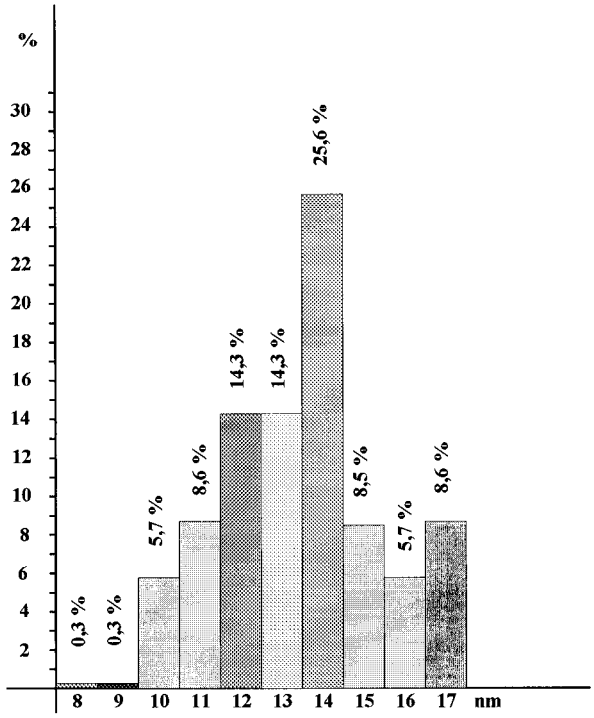

Figure 6. Ni particle size distribution of Ni·4TiO_2 (**12a(o)**), prepared from $Ni(OAc)_2$ and $Ti(OEt)_4$ (without lysine).

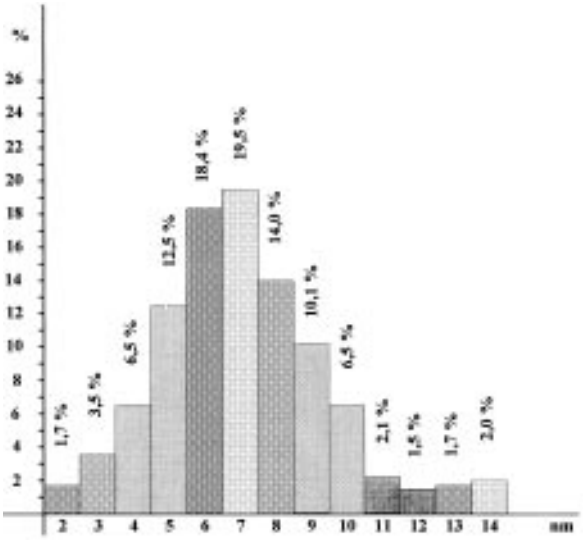

Figure 7. Ni particle size distribution of Ni·4ZrO_2 (**12b)**, prepared from $Ni(OAc)_2$ and $(PrO)_3$Zr(lysinate).

Preparation of $M(OR)_3$(lysinate). *[$Ti(OEt)_3$(lysinate)]$_2$ (**1a**):* Lysine (1.46 g, 10 mmol) was added to an ethanolic (50 mL) solution of $Ti(OEt)_4$ (2.28 g, 10 mmol). While the suspension was stirred at room temperature for 2 h, the lysine dissolved. After removal of the solvent in vacuo, a yellowish solid was obtained. IR (Nujol) 3270 (m,NH), 3125 (br, NH), 1644 (vs, CO), 1146 (s, C−OEt terminal), 1098 (s, C−OEt terminal), 1066 (sh, C−OEt terminal), 1051 (sh, C−OEt bridging), 905 (s, C−OEt terminal), 879 (m, C−OEt bridging), 659 (m, C−OEt terminal), 559 (m, C−OEt terminal) cm^{-1}. ^{13}C NMR (200 MHz, CD_3OD, δ) 184.0 (COO), 79.5 (CH), 58.3 ($TiOCH_2$), 41.4, 34.4, 31.1, 24.3 (CH_2, lysinate), 18.4 (CH_3).

*[$Zr(OPr)_3$(lysinate)]$_x$ (**1b**):* Lysine (1.46 g, 10 mmol) was added to an propanolic (50 mL) solution of $Zr(OPr)_4$ (4.68 g, 10 mmol). When the suspension was heated to 60 °C, the lysine dissolved. After removal of the solvent in vacuo, a yellowish solid was obtained. IR (Nujol) 3268 (m, NH), 1640

Table 9. JCPDS *d* Spacings for Comparison (Int > 2; *d* > 1.4)

anatase	rutile	$CoTiO_3$	$NiTiO_3$	CuO	ZrO_2	Co	Ni	Cu
3.52	3.247	3.717	4.598	2.758	2.93	2.0467	2.034	2.088
2.431	2.487	2.727	3.685	2.531	2.55	1.7723	1.762	1.808
2.378	2.297	2.534	2.705	2.524	1.801			
2.332	2.188	2.3202	2.516	2.311	1.534			
1.892	2.054	2.224	2.332	1.9608	1.471			
1.6999	1.6874	2.0934	2.299	1.8667	1.27			
1.6665	1.6237	1.8566	2.207	1.7124	1.167			
1.493	1.4797	1.8114	2.077	1.5811	1.135			
1.4808	1.4528	1.7114	1.8417	1.5055				
		1.6178	1.6962					
		1.614	1.6025					
		1.4974	1.4859					
		1.4628	1.4522					

(vs, CO), 1614 (s), 1532 (m), 1336 (m), 1076 (m), 540 (m) cm^{-1}. Anal. Calcd for $C_{15}H_{34}N_2O_5Zr$: C, 43.6; H, 8.2; N, 6.8. Found: C, 41.9; H, 8.5; N, 6.6.

For all subsequent reactions, ethanolic solutions of $M(OR)_3$-(lysinate) were used without removal of the solvent.

Preparation and Sol−Gel Processing of the Complexes 2−4. $Ni(OAc)_2$, $Co(OAc)_2$, or $Cu(OAc)_2 \cdot H_2O$ (2.5 mmol) was added to a freshly prepared solution of **1** (10 mmol) in 400 mL of ethanol. In the reaction with the copper salt, acetic acid (10 mmol) was added before the metal salt. The suspensions were heated to 60 °C until the metal salt was completely dissolved. Deeply colored solutions were obtained. The UV maxima are given in the Results Section.

Water (4.05 mL, 225 mmol) was then added to the solution of **2** and **3**, and 2.7 mL (150 mmol) to the solution of **4**. The clear solutions were stirred at 60 °C for 72 h. During this period they turned slightly turbid. The solvent was then removed at 70 °C/3 kPa. The obtained xerogels **5**−**7** were dried at 0.1 Pa.

5a: Anal. Calcd for $C_{28}H_{58}CoN_8O_{18}Ti_4$: C, 32.2; H, 5.6; N, 10.7; Co, 5.6; Ti, 18.3. Found: C, 33.3; H, 5.9; N, 8.7; Co, 5.4; Ti, 16.7. Specific surface area 0.5 m^2/g.

6a: Anal. Calcd for $C_{28}H_{58}N_8NiO_{18}Ti_4$: C, 32.2; H, 5.6; N, 10.7; Ni, 5.6; Ti, 18.3. Found: C, 31.8; H, 5.6; N, 10.0; Ni, 4.7; Ti, 17.3. Specific surface area 4.0 m^2/g.

7a: Anal. Calcd for $C_{36}H_{70}CuN_8O_{24}Ti_4$: C, 34.5; H, 5.6; N, 8.9; Cu, 5.1; Ti, 15.3. Found: C, 38.1; H, 7.3; N, 8.5; Cu, 4.9. Specific surface area <0.1 m^2/g.

5b: Anal. Calcd for $C_{28}H_{58}CoN_8O_{18}Zr_4$: C, 27.6; H, 4.8; N, 9.2. Found: C, 28.2; H, 4.5; N, 6.3.

6b: Anal. Calcd for $C_{28}H_{58}N_8NiO_{18}Zr_4$: C, 27.6; H, 4.8; N, 9.2. Found: C, 27.3; H, 5.2; N, 7.2. Specific surface area <0.1 m^2/g.

7b: Anal. Calcd for $C_{36}H_{70}CuN_8O_{24}Zr_4$: C, 30.3; H, 4.9; N, 7.9. Found: C, 29.9; H, 5.3; N, 5.6. Specific surface area <0.1 m^2/g.

Sol−Gel Processing of Unmodified $M(OR)_4$ in the Presence of Metal Acetates. Water (5.4 mL, 300 mmol) was added to the solutions of $Ti(OEt)_4$ or $Zr(OEt)_4$ (10 mmol) and $Ni(OAc)_2$, $Co(OAc)_2$, or $Cu(OAc)_2 \cdot H_2O$ (2.5 mmol) in ethanol (400 mL). The clear solutions were stirred at 60 °C for 72 h. During this period they turned slightly turbid. The solvent was then removed at 70 °C/3 kPa. The obtained xerogels **5-(o)**−**7(o)** were dried at 0.1 Pa.

5a(o): Anal. Calcd for $C_4H_6CoO_{12}Ti_4$: C, 9.7; H, 1.2; Co, 11.9; Ti, 38.6. Found: C, 15.6; H, 3.5; Co, 10.7; Ti, 36.8.

6a(o): Anal. Calcd for $C_4H_6NiO_{12}Ti_4$: C, 9.7; H, 1.2; Ni, 11.8; Ti, 38.6. Found: C, 17.2; H, 3.7; Ni, 10.2; Ti, 36.9.

7a(o): Anal. Calcd for $C_4H_6CuO_{12}Ti_4$: C, 9.6; H, 1.2; Cu, 12.7; Ti, 38.2. Found: C, 15.8; H, 3.3; Cu, 10.7; Ti, 34.1.

5b(o): Anal. Calcd for $C_4H_6CoO_{12}Zr_4$: C, 7.2; H, 0.9; Co, 8.8. Found: C, 11.1; H, 2.5; Co, 6.2.

6b(o): Anal. Calcd for $C_4H_6NiO_{12}Zr_4$: C, 7.2; H, 0.9; Ni, 8.8. Found: C, 11.5; H, 2.8; Ni, 5.5.

7b(o): Anal. Calcd for $C_4H_6CuO_{12}Zr_4$: C, 7.1; H, 2.6; Cu, 9.4. Found: C, 11.8; H, 2.6; Cu, 6.6.

Oxidation of the Metal-Complex-Containing Gels. The polycondensates **5**−**7** or **5(o)**−**7(o)** were placed in a horizontal quartz tube, heated in an tube oven to 500 °C by 10 °C/min, and then held at 500 °C for 2 h. A stream of 1 L/min dry air was maintained during heating. Elemental analysis of the products showed that carbon, hydrogen, and nitrogen are completely removed (C, H, N values < 0.3%).

8a: Anal. Calcd for CoO_9Ti_4: Co, 14.9; Ti, 48.6. Found: Co, 13.7; Ti, 44.8.

9a: Anal. Calcd for NiO_9Ti_4: Ni, 14.9; Ti, 48.6. Found: Ni, 13.5; Ti, 51.9. Specific surface area 45 m^2/g.

10a: Anal. Calcd for CuO_9Ti_4: Cu, 15.8; Ti, 48.0. Found: Cu, 14.0; Ti, 48.5.

8b: Anal. Calcd for CoO_9Zr_4: Co, 10.3. Found: Co, 8.2.

9b: Anal. Calcd for NiO_9Zr_4: Ni, 10.3. Found: Ni, 7.0.

10b: Anal. Calcd for CuO_9Zr_4: Cu, 11.1. Found: Cu, 9.7.

8a(o): Anal. Calcd for CoO_9Ti_4: Co, 14.9; Ti, 48.6. Found: Co, 13.9; Ti, 43.1.

9a(o): Anal. Calcd for NiO_9Ti_4: Ni, 14.9; Ti, 48.6. Found: Ni, 14.1; Ti, 52.8.

10a(o): Anal. Calcd for CuO_9Ti_4: Cu, 15.8; Ti, 48.0. Found: Cu, 13.4; Ti, 35.9.

8b(o): Anal. Calcd for CoO_9Zr_4: Co, 10.3. Found: Co, 8.5.

9b(o): Anal. Calcd for NiO_9Zr_4: Ni, 10.3. Found: Ni, 8.0.

10b(o): Anal. Calcd for CuO_9Zr_4: Cu, 11.1. Found: Cu, 9.6.

Reduction of the Oxidic Composites. The composites **8**−**10** or **8(o)**−**10(o)** were placed in a horizontal quartz tube flushed with argon. While a stream of hydrogen of 200 mL/min was maintained, the samples were heated to 500 °C by 10 °C/min, held them at 500 °C for 2 h and then cooled to room temperature. Before opening the apparatus, it was flushed with argon.

11a: Anal. Calcd for CoO_8Ti_4: Co, 15.5. Found: Co, 13.7.

12a: Anal. Calcd for NiO_8Ti_4: Ni, 15.4; Ti, 50.6. Found: Ni, 14.7; Ti, 51.3.

13a: Anal. Calcd for CuO_8Ti_4: Cu, 16.5; Ti, 50.1. Found: Cu, 14.9; Ti, 48.7.

11b: Anal. Calcd for CoO_8Zr_4: Co, 10.7. Found: Co, 9.3.

12b: Anal. Calcd for NiO_8Zr_4: Ni, 10.7. Found: Ni, 8.2.

13b: Anal. Calcd for CuO_8Zr_4: Cu, 11.4. Found: Cu, 10.3.

11a(o): Anal. Calcd for CoO_8Ti_4: Co, 15.5. Found: Co, 14.8.

12a(o): Anal. Calcd for NiO_8Ti_4: Ni, 15.4; Ti, 50.6. Found: Ni, 14.7; Ti, 51.3.

13a(o): Anal. Calcd for CuO_8Ti_4: Cu, 16.5; Ti, 50.1. Found: Cu, 15.8; Ti, 53.1.

11b(o): Anal. Calcd for CoO_8Zr_4: Co, 10.7. Found: Co, 9.0.

12b(o): Anal. Calcd for NiO_8Zr_4: Ni, 10.7. Found: Ni, 8.2.

13b(o): Anal. Calcd for CuO_8Zr_4: Cu, 11.4. Found: Cu, 9.8.

Acknowledgment. This work was supported by the Deutsche Forschungsgemeinschaft, the Fonds der Chemischen Industrie, and the Volkswagen Foundation. We thank Dr. A. Kaiser and Dr. J. Schulz, Fraunhofer-Institut für Silicatforschung Würzburg, for their help in obtaining the XRD and solid-state UV spectra.

CM960162N